Smart Structures and Systems, *Vol. 32*, *No. 2* (*2023*) *123-133*
https://doi.org/10.12989/sss.2023.32.2.123

Thermography-based coating thickness estimation for steel structures using model-agnostic meta-learning

Jun Lee [1a], Soonkyu Hwang [2b], Kiyoung Kim [1b] and Hoon Sohn[*1]

[1] *Department of Civil Engineering, Korean Advanced Institute for Science and Technology, 291 Daehak-ro, Yuseong-gu, Daejeon 34141, Republic of Korea*
[2] *Yield Enhancement Team, Global Infra Technology, Samsung Electronics, Asan 31489, South Korea*

(*Received November 24, 2022, Revised July 4, 2023, Accepted July 20, 2023*)

Abstract. This paper proposes a thermography-based coating thickness estimation method for steel structures using model-agnostic meta-learning. In the proposed method, a halogen lamp generates heat energy on the coating surface of a steel structure, and the resulting heat responses are measured using an infrared (IR) camera. The measured heat responses are then analyzed using model-agnostic meta-learning to estimate the coating thickness, which is visualized throughout the inspection surface of the steel structure. Current coating thickness estimation methods rely on point measurement and their inspection area is limited to a single point, whereas the proposed method can inspect a larger area with higher accuracy. In contrast to previous ANN-based methods, which require a large amount of data for training and validation, the proposed method can estimate the coating thickness using only 10- pixel points for each material. In addition, the proposed model has broader applicability than previous methods, allowing it to be applied to various materials after meta-training. The performance of the proposed method was validated using laboratory-scale and field tests with different coating materials; the results demonstrated that the error of the proposed method was less than 5% when estimating coating thicknesses ranging from 40 to 500 μm.

Keywords: coating thickness evaluation; model-agnostic meta-learning; non-destructive test; steel structure; thermography

1. Introduction

Coatings are widely used to protect steel structures from corrosion, abrasion, cracking, etc. (Standard 2012, Shrestha and Kim 2017a); however, it has been challenging to control the coating thickness during its application on a structure. A coating layer thinner than the required thickness is more prone to corrosion, whereas a thicker one increases costs as well as the weight of the steel structure. Furthermore, a thicker coating layer is more vulnerable to internal stress in the coating caused when the surface shrinks more quickly than the inner coating material. In addition, the coating layer thins and deteriorates with time, which can lead to defects of coating, such as corrosion, delamination, chalking, checking, and so on (A.A.o.S.a.H.T. Officials 2019, I.a.T.o.S.K. Ministry of Land 2019, Ochiai *et al*. 2007).

Currently, the coating thickness of steel structures is inspected manually using contact-type sensors, such as eddy current sensors, magnetic induction sensors, and Hall effect sensors (Cheng 2017, Shen *et al*. 2013). Even though contact-type sensors have a high resolution of approximately 5 μm, measurements need to be repeated multiple times to cover a large inspection area because a single measurement is only localized at one location. Further, the changing contact conditions between the sensor and the target surface can also result in a significant error in the coating thickness estimation.

Thus, to address the limitations of contact-type sensors, several cutting-edge solutions based on ultrasonics, terahertz, and X-ray fluorescence have been developed to accurately and practically measure coating thickness. Ultrasonic (Beamish 2004, Zhang *et al*. 2021) and terahertz (Russe *et al*. 2012) methods can be used to precisely measure the thickness of a material using its refractive index. However, similar to contact-type sensors, they can only measure one point on the material surface at a time, and their applicability is restricted because the humidity and temperature of the transmission media have a significant impact on the velocity and frequency of ultrasonic waves. The X-ray fluorescence method (Giurlani *et al*. 2019) does not require reference data for precise coating thickness estimation; however, its widespread application has been hindered by the massive size of the equipment required and the restricted size of the specimens.

To estimate the coating thickness over a large area, the simulation of the infrared thermography is experimented using finite element method (Shrestha and Kim 2017). Two different thermography methods are used for estimating the coating thickness. Also, a thermography based coating estimation was explored. A white halogen lamp, which has been frequently employed as the heat source (Bu *et al*.

*Corresponding author, Ph.D., Professor,
E-mail: hoonsohn@kaist.ac.kr
[a] Ph.D. Student
[b] Ph.D.

ISSN: 1738-1584 (Print), 1738-1991 (Online)

2016, Zhang *et al*. 2016), applied heat flux to a target surface, and the corresponding heat responses were captured as a two-dimensional image (Moskovchenko *et al*. 2020). And, a coating thickness non-uniformity is measured using flash pulse thermography (Muzika and Švantner 2020). The relationship between phase angle of thermography and coating thickness is calculated and the Those analytical modeling and study revealed that the coating thickness is proportional to the thermal effusivity of the structure. However, the thermal effusivity measurement is affected by the inconsistent heating of the halogen lamp, which degrades the accuracy of the coating thickness measurement.

Recently, machine learning methods have been applied to thermographic data to enhance the accuracy and reduce the computational time required for coating thickness estimation. For example, an artificial neural network (ANN) was applied to thermographic data collected from non-metallic structures under a continuous constant heat source (Wang *et al*. 2016). The study showed the possibility of coating thickness estimation without the thermal properties of a coating and structure by introducing an ANN but did not tackle the problems that can be caused by the preconditions of ANN training. Because training an ANN requires a large amount of data, and the trained ANN is optimized for a specific task (Chauchard *et al*. 2004), it is difficult to use ANNs in similar but different tasks, such as for analyzing different coating material types, coating colors, or thickness ranges.

In this study, a coating thickness estimation method based on model-agnostic meta-learning was proposed. The proposed method uses a halogen thermography system, in which a halogen lamp transmits heat over a broad area of a structure and an infrared (IR) camera captures a series of thermal images. The proposed method employs meta-learning, which learns training methods by training on a variety of similar tasks, thereby enabling the rapid optimization of new tasks with minimal data. By utilizing meta-learning, the proposed method achieves a high degree of accuracy with a small amount of data from different coating materials. The proposed method (1) estimates the coating thickness of a larger area more accurately than the previous methods; (2) requires minimal-sized devices that can be applied in the field without significant external environmental influence; and (3) requires a small sample size (less than 10) to estimate the coating thickness and can be easily applied to other coating materials.

The remainder of this paper is organized as follows. An overview of the proposed coating thickness estimation method is provided in Section 2. Section 3 describes the meta-learning used in the proposed method in detail and the experimental validation. The concluding remarks are presented in Section 4.

2. Meta-learning-based coating thickness estimation network method (Meta-CTEN)

This section describes the model-agnostic meta-learning-based coating thickness estimation method (Meta-CTEN), which can be applied to any coating material. The proposed method consists of two parts: a halogen thermography monitoring system and a meta-learning-based coating thickness estimation network (Meta-CTEN). The halogen thermography monitoring system, its components, and operation procedures are described in detail in Section 2.1. In Section 2.2, the concept of meta-learning is offered for the comprehension of readers, and CTEN, the baseline network for the proposed coating thickness estimation method based on meta-learning, is proposed in Section 2.3.

2.1 Halogen thermography system for monitoring

Fig. 1 shows the halogen thermography system adopted in the proposed method and its working procedure. The system is composed of three devices for heating, sensing, and control. A halogen lamp, which generates heat energy on the target surface, is placed at the center of the target structure. An infrared (IR) camera captures a series of IR images that visualize the resulting heat responses of the target surface within its field of view (FOV). To avoid measuring the halogen light reflected from the target structure, the IR camera is mounted at an angle of 10 to 15° from the normal line of the target structure. The controller operates by turning the halogen lamp on and off, transmitting control signals to the IR camera, and receiving real-time IR images from the IR camera to estimate the coating thickness.

Although the halogen lamp has a significant shortcoming mentioned in the introduction, that is, its inability to evenly distribute heat over a large area, the proposed system uses a halogen lamp as the heating device. While the halogen lamp has resulted in a significant thickness measurement error in the previous coating thickness estimation methods, the machine learning technique in the proposed method can minimize the error caused by the non-uniform excitation because it deals with time series data for each pixel. The halogen thermography system used in the proposed method has the additional advantage of efficiently estimating coating thickness over a large area.

In the proposed halogen thermography system, the halogen lamp repeatedly turns on and off at a specific period with respect to an ON/OFF-type excitation signal, as shown in Fig. 2(a). The monitoring time is divided into the

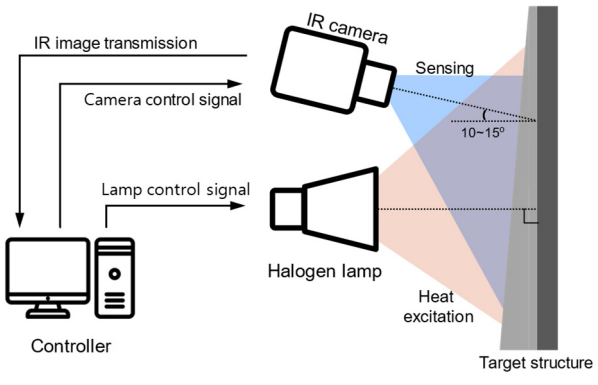

Fig. 1 Overview of the proposed halogen thermography system for coating thickness estimation

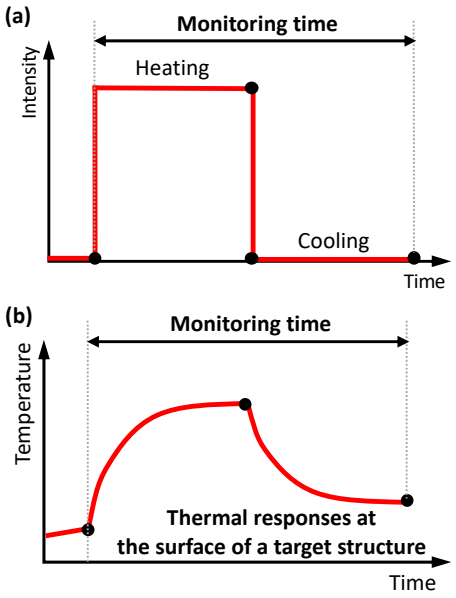

Fig. 2 (a) Excitation signal transmitted to the halogen lamp; and (b) the heat response corresponding to the external heating unit

heating and cooling phases, and the durations of the phases are set to be identical in the proposed method. The temperature at a specific pixel point then increases and decreases in the heating and cooling phases, respectively, as shown in Fig. 2(b). Because the temperature change of the target structure should be discerned by the IR camera in each measurement, the length of the monitoring time can be adjusted such that the surface temperature of the target structure increases by at least 3°C in the test environment.

The controller in the proposed halogen thermography system transmits control signals to the halogen lamp and camera and collects thermal image data. First, the controller determines the monitoring time considering the test environment and transmits the lamp operation signal to the halogen lamp and the IR camera simultaneously. Then, the halogen lamp turns on and off in response to the controller's signal and radiates heat to the surface of the target structure, while the IR camera captures the thermal changes of the target structure in succession. The thermal images captured by the IR camera are transferred to the controller and pre-processed to generate the input data, which is utilized by the proposed method for coating thickness estimation.

2.2 Concept of meta-learning

Advance computing technologies such as pattern recognition (Farrar and Worden 2012, Flah *et al*. 2021), knowledge-based systems (Darban *et al*. 2020), and machine learning (Avci *et al*. 2022, Goulet 2020, Reich 1997) have expanded their applications in structural health monitoring (SHM) in civil engineering. However, because a typical machine learning algorithm is trained for a single task requiring particular structures or materials, it is challenging to apply the algorithm to a different task using different structures or materials. In addition, the machine learning algorithm used in SHM applications should be able to learn and adjust quickly from a small sample of data and continue to make adjustments as more data becomes available.

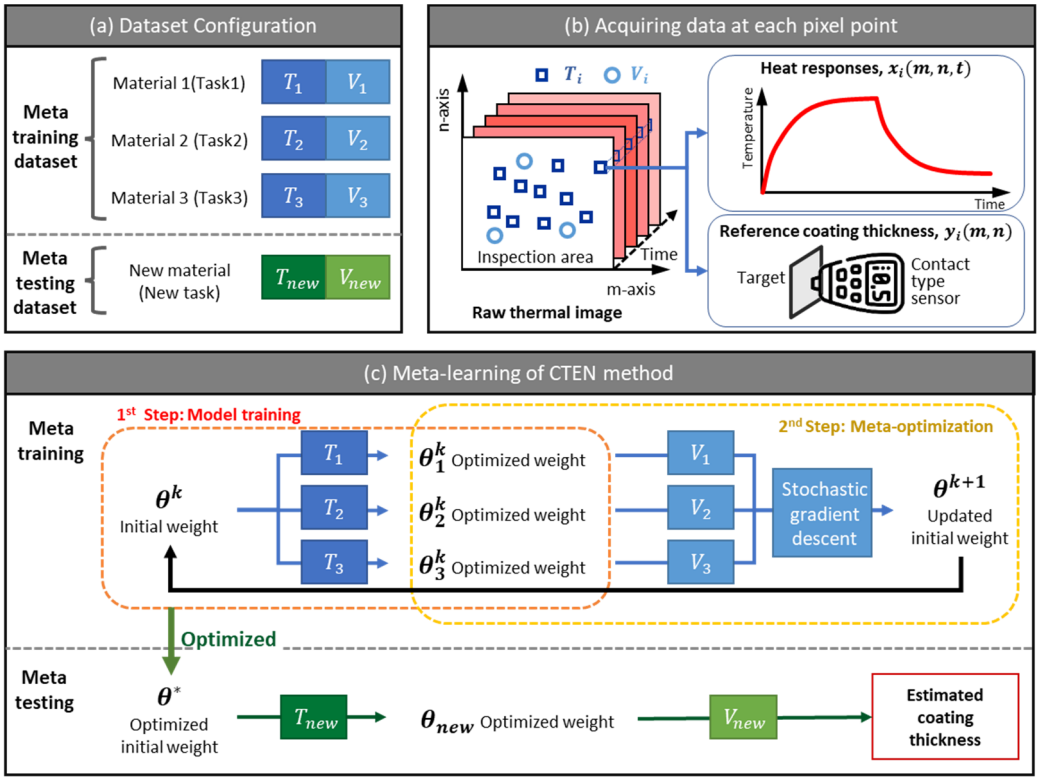

Fig. 3 Overview of the proposed coating thickness estimation method

Meta-learning is one approach to address the aforementioned issues with machine learning applied to SHM applications. It refers to a machine learning algorithm that learns from the output of other machine learning algorithms to produce its own predictions. The objective of meta-learning is to train a baseline network that can rapidly adapt to a new task using only a few training pixel points and iterations.

Fig. 3 illustrates the application of meta-learning to the proposed method for estimating coating thicknesses. Meta-learning consists of meta-training and meta-testing, as shown in Fig. 3(a). The meta-training dataset for the ith target structure ($i = 1,2,\cdots,M$) consists of a training dataset and a validation dataset, denoted as T_i and V_i, respectively. As depicted in Fig. 3(b), T_i and V_i consist of the time history of the heat response x_i(m,n,t) measured by the IR camera and the reference (ground-truth) coating thickness $y_i(m,n)$ measured by a contact-type sensor, where (m,n) is the coordinate of a pixel point. The number of the pixel points can be defined by a user, and $x_i(m,n,t)$ and $y_i(m,n)$ at each pixel point are used as input and output data, respectively. The meta-testing dataset basically has the same structure as the meta-training dataset, except that the meta-testing dataset is constructed from a new different material and $y_{new}(m,n)$ of V_{new} are not collected.

The meta-learning of the CTEN model in the proposed method consists of two steps: meta-training and meta-testing, as shown in Fig. 3(c). The meta-training step consists of model training and meta-optimization. In model learning, similar to the current learning algorithms, an initial weight θ^k is trained using T_i through the kth iteration to be updated to θ_i^k, which is an optimized weight for each target structure from 1 to M. In meta-optimization, θ_i^k is updated to θ^{k+1} by conducting stochastic gradient descents on all target structures. In the meta-testing step, the optimal initial weight θ^* is obtained through iterative updates of θ^k; then, θ^* is used to complete the coating thickness estimation model with limited data obtained from target structures made of a new material. The details of meta-learning of the CTEN model are discussed in Sections 2.3 and 2.4.

2.3 Coating thickness estimation network (CTEN)

As illustrated in Fig. 4, CTEN is constructed with one-dimensional convolution (1D Conv) layers and fully connected layers. The 1D Conv layers are composed of three distinct convolution layers with batch normalization and a rectified linear unit (ReLU) activation function (Hahnloser *et al*. 2000). 10 kernels with a 1 × 5 window, 20 kernels with a 1 × 3 window, and 25 kernels with a 1 × 3 window are used for the first, second, and third convolutional layers, respectively. The number of strides and padding are 2 and 2 for the first layer, 1 and 1 for the second layer, and 1 and 1 for the third layer. Average pooling was applied with a 1 × 2 window and stride of 2 after the first and second convolution layers, and a 1 × 3 window and stride of 3 after the third convolution layer. Finally, a single-node output regression layer is included after the dense layers.

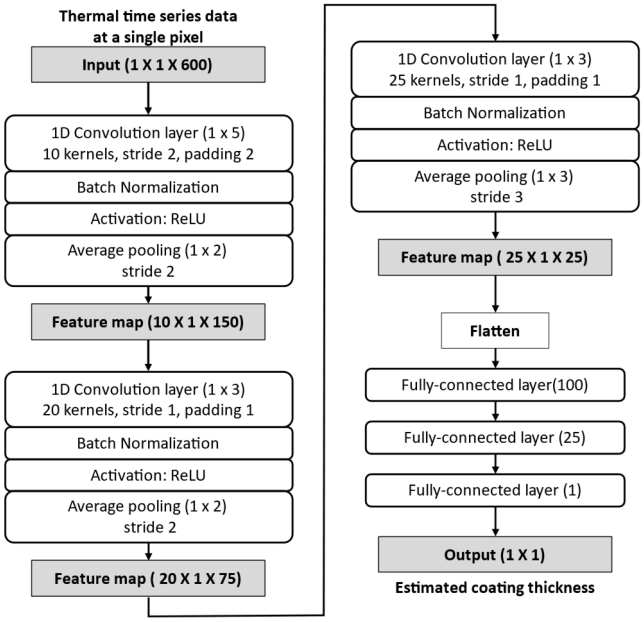

Fig. 4 Overview of Coating Thickness Estimation Network (CTEN)

The loss function $L(\theta, T_i)$ is defined as the squared L2 norm between the estimated and reference coating thicknesses, as expressed in Eq. (1)

$$L(\theta, T_i) = \sum_{x_i, y_i \sim \mathcal{T}_i} \| f_\theta(x_i) - y_i \|_2^2 \tag{1}$$

2.4 Model-agnostic meta-learning-based coating thickness estimation method

The meta-learning of the CTEN model, which is an optimization-based meta-learning(Finn, Abbeel, and Levine 2017), used in the proposed method is depicted in Fig. 5. First, the CTEN's optimized weights for the ith coating material become the updated weight parameters θ_i^k after adapting to T_i and training the CTEN. In this process, θ_i^k is computed using gradient descent updates on T_i, as shown in Eq. (2)

$$\theta_i^k \leftarrow \theta^k - \alpha \nabla L(\theta^k, T_i) \tag{2}$$

where α is the network step size. To validate θ_i^k for each material, $L(\theta_i^k, V_i)$ in Equation (1) is calculated using θ_i^k and V_i. The variable θ^k is defined as the optimized initial weight θ^* when $L(\theta_i^k, V_i)$ is lower than or equal to the learning threshold ε for all the training materials.

When $L(\theta_i^k, V_i)$ is higher than the learning threshold ε, θ^k is updated to θ^{k+1} using the optimization of meta-learning across tasks through the gradient descent expressed in Eq. (3)

$$\theta^{k+1} \leftarrow \theta^k - \beta \nabla \sum L(\theta_i^k, V_i) \tag{3}$$

where β is the meta step size. By iterating the process in

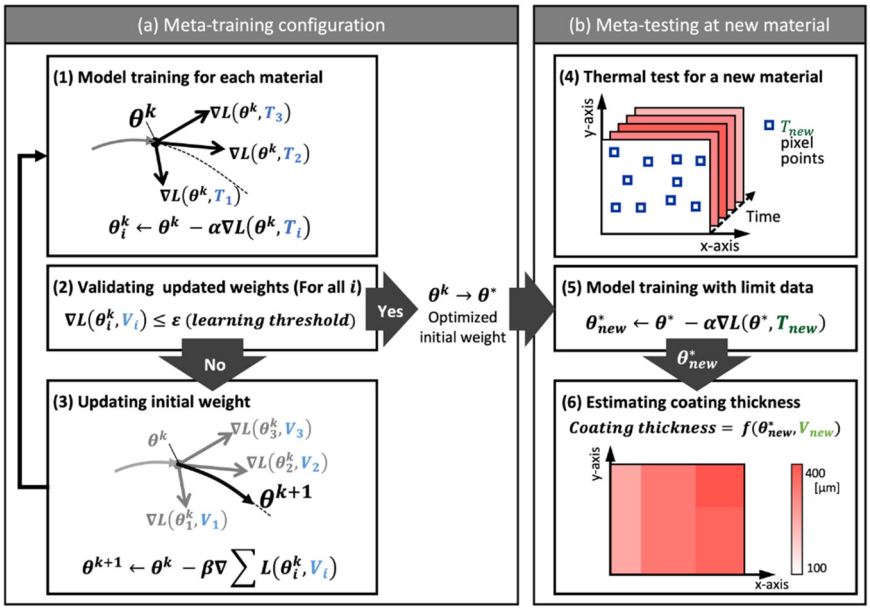

Fig. 5 Overview of coating thickness estimation based on model agonistic meta-learning

Eq. (3), the network can configure the initial weight θ^k more generally than each task, and optimize each task with only a small number of pixel points. The result of meta-training is the optimized initial weight θ^*.

Meta-testing is a procedure for estimating the coating thickness of a new material, as illustrated in Fig. 5(b). In meta-testing, the coating thickness estimation is trained with T_{new} using θ^*. First, several pixel points are randomly chosen, and the reference coating thickness is measured at the same pixel points in a thermal test of the new material. Subsequently, CTEN is trained to obtain θ_{new}^*, which is used in CTEN with thermal data at each pixel point V_{new} to estimate the coating thickness of the new material.

3. Meta-training and validation of Meta-CTEN

Laboratory-scale and field tests were performed to verify the performance of the proposed method. Input and output data were collected using the halogen thermography system explored in Section 2.1 and applied to the training process for meta-learning of the proposed method, as described in Section 3.1. The accuracy of the proposed method was validated through a lab-scale test, as described in Section 3.2, and its applicability was assessed via the field test, as described in Section 3.3.

3.1 Meta-training of Meta-CTEN

Fig. 6 shows the setup of the proposed halogen thermography system for collecting thermal data. An InfraTec VarioCAM hr head IR camera with a spatial resolution of 480 × 640 pixels was adopted in this test. The temperature resolution and spectral range of the IR camera are 0.03 K and 7.5 μm, respectively. The FOV of the IR camera was expanded to 65° × 51° by mounting a Jenoptic wide-angle lens. A Hedler H25s 3400 W halogen lamp was

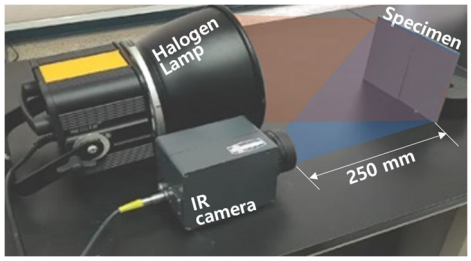

Fig. 6 Configuration of the halogen thermography system for lab-scale experiment

adopted as the heat source of the proposed system. The distance from the IR camera lens and halogen lamp to the surface of the specimens was set to 250 mm in the test. A control software was used to adjust the light intensity and the heating and cooling times of the halogen lamp. In this case, the heating and cooling times were set to 5 s each.

To measure the reference coating thickness of the target structures, a DUALSCOPE MP0R-FPW contact-type magnetic induction sensor (Fig. 7(a)) was used at multiple points to construct a reference coating thickness image (Fig. 7(b); (Hwang *et al.* 2022)). The accuracy of the magnetic induction sensor is up to 3 μm, whereas its spatial measurement range is restricted to 10 mm. To enhance the pixel resolution of the reference coating thickness image, linear interpolation was applied using a pixel magnification factor P. Although the number of pixels in the linearly interpolated reference coating thickness image remains the same as in the thermal image, the actual resolution is increased P times owing to the sparse measurement density, as shown in Fig. 7(b).

Fig. 8 shows the meta-training specimens of the target structures. The base material of the specimens is SS-400 steel, and two coating materials – epoxy and urethane – were applied to the surface of the specimen. The epoxy coating shown in Fig. 8(a) was applied with varying

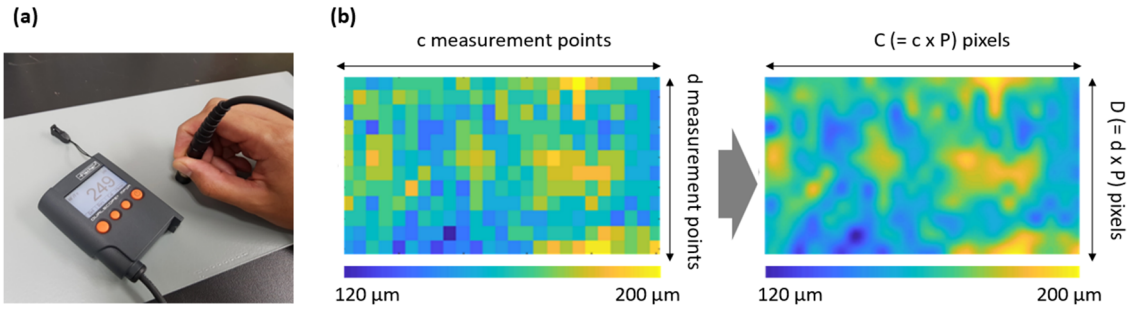

Fig. 7 Construction of the reference coating thickness at each pixel point: (a) measuring coating thickness using a contact-type sensor; (b) interpolation-based reference coating thickness at each pixel point

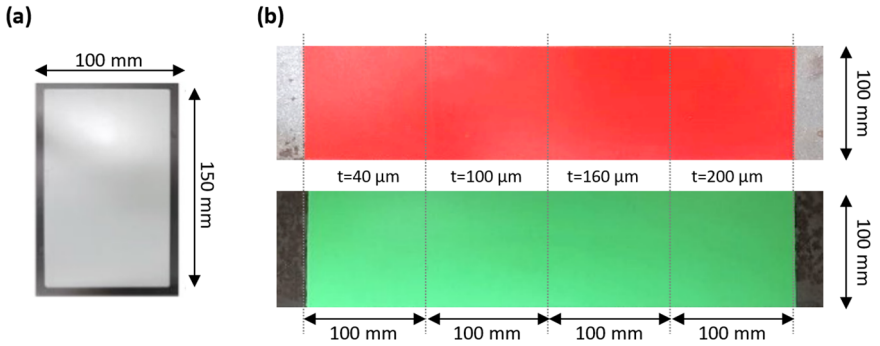

Fig. 8 Meta-learning training specimen: (a) training structure coated with gray-colored epoxy; and (b) red-colored and light-green–colored urethane

thicknesses (50, 200, 300, 400, 550, and 700 μm). Fig. 8(b) shows the specimens coated with two types of urethanes, distinguishable by their red and light green colors. The thicknesses of the urethane coatings are 40, 100, 160, and 200 μm. Also, the emissivity of the two coating materials is in the range of 0.90 to 0.95 approximately.

The Meta-CTEN method was implemented based on the Pytorch framework (Paszke *et al*. 2019) and deployed on a workstation equipped with an Intel Core i7-9700 CPU, 32 GB DDR4 RAM, and an NVIDIA Titan 12 GB GPU. In addition, the Adam optimizer (Kingma and Ba 2015) was used for model optimization. The hyperparameters in this method were selected using grid search. To prevent overfitting due to excessive repetitive training, the error in the training results was continuously monitored for each epoch, and the training was terminated if the loss did not diminish within five epochs.

3.2 Lab-scale test

In the lab-scale test, two plate-type specimens were fabricated using SS-400 steel for meta-training and meta-testing. The thickness of the base material was 10 mm, and the height and width were 100 mm and 400 mm, respectively, as shown in Fig. 9. The specimens for meta-training were coated with a green-colored epoxy coating material (Fig. 9(a)) and white-colored acrylic coating material (Fig. 9(b)). The specimens were coated with thicknesses of 80, 120, 160, and 200 μm, and the reference coating thickness was measured using a contact-type sensor.

To validate the accuracy of the proposed Meta-CTEN method with respect to the number of pixel points, two training scenarios with 5- and 10-pixel points were conducted. Also, the performance of the proposed Meta-CTEN was validated by comparing it with a transfer learning method used to solve similar tasks (Pan and Yang 2010) and a common machine learning method. When a new task has a small dataset, the transfer learning method, referred to as Pr-CTEN in this paper, utilizes a portion of the pretrained model for similar tasks, and only the final layer is fine-tuned to fit the new task. The Pr-CTEN model was trained using T1–T3 from each meta-training dataset, followed by fine-tuning with T_{new} from the meta-testing dataset. 10- or 100-pixel points were used to train Pr-CTEN using the test specimens. The common machine learning method, referred to as Tr-CTEN, which is typically used in a single task with a single test specimen, was also utilized to validate the learning accuracy of the proposed meta-learning. In the lab-scale test, Tr-CTEN was purposefully well-trained for each coating material specimen so that it had better accuracy than Meta-CTEN and Pr-CTEN. Tr-CTEN was trained using a meta-testing dataset with 10,000-pixel points for each specimen. So, the results of Tr-CTEN are used for reference data.

During fine-tuning of the model by meta-learning, each gradient step was computed using the same pixel points. The accuracy of the two methods was expressed with numerical data using the mean absolute error (MAE) in Eq. (4)

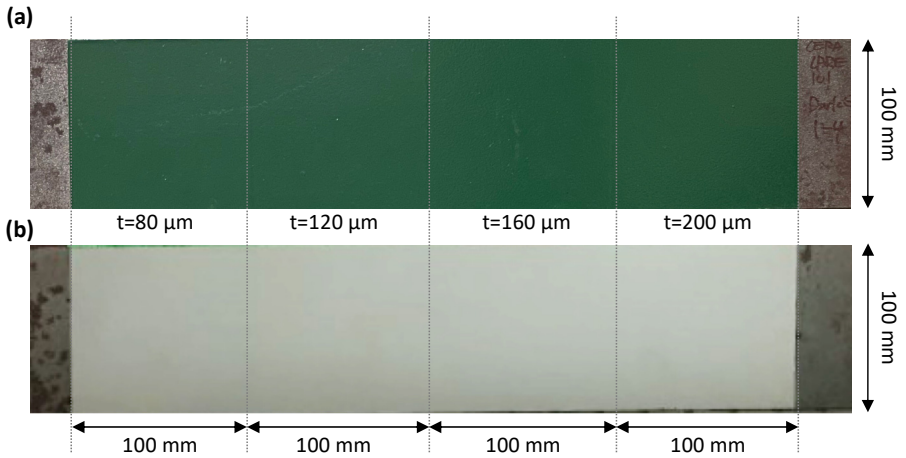

Fig. 9 Specimens coated with different coating material (thickness: 80–200 um): (a) green-colored epoxy type; (b) white-colored acrylic type

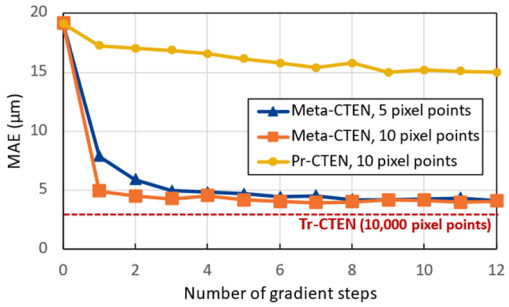

Fig. 10 Quantitative coating thickness estimation results showing the learning curve at meta test of acrylic coating material

$$MAE(\mu m) = \frac{1}{N_{V_{new}}} \sum_{x,y \sim V_{new}} |f_{\theta^*}(x) - y| \tag{4}$$

where $N_{V_{new}}$ is the total number of pixel points in V_{new}. In addition, the relative error is defined in Eq. (5) to determine the magnitude of MAE in terms of the reference measurement

$$E_{est}(\%) = \frac{100}{N_{V_{new}}} \sum_{x,y \sim V_{new}} \frac{|f_{\theta^*}(x) - y|}{y} \tag{5}$$

Fig. 10 shows the validation machine learning curve for the acrylic coating material specimen. Despite being trained for maximum performance after only three gradient steps, the MAE of Meta-CTEN is close to the results for Tr-CTEN and the meta- CTEN trained using meta-learning continues to improve with subsequent gradient steps. In addition, rather than overfitting to parameters that only improve after one step, the Meta-CTEN model optimizes the parameters such that they reside in a zone that is receptive to quick adaptation and sensitive to the loss function from the meta-training dataset.

Table 1 shows the error in evaluation of coating thickness. The well-trained Tr-CTEN shows the lowest MAE and E_{est} as expected. Further, the MAEs of the proposed Meta-CTEN based method are only 21.3% and 12.2% higher than those of Tr-CTEN, indicating that the proposed method can demonstrate comparable performance to Tr-CTEN only with 0.1% of pixel points that Tr-CTEN requires. In comparison, Pr-CTEN presents two times more inaccurate results even though it used 100 pixel points in training. On the contrary, Meta-CTEN is more stable than Pr-CTEN in terms of the accuracy difference between different coating materials. In the test using 10 pixel points, the difference of E_{est} in the proposed method is only 0.03%; however, Pr-CTEN shows a 3.52% difference, which indicates that the proposed method is applicable regardless of the type or color of coating material.

Fig. 11 shows the results of the thickness estimation for white-colored acrylic coating. Even though the number of pixel points used in the training of Meta-CTEN is only 10% of that of Pr-CTEN, the visualized result of Meta-CTEN

Table 1 Estimation error of the coating thickness on the test specimens

Model	MAE (μm)		E_{est} (%)	
	Epoxy type	Acrylic type	Epoxy type	Acrylic type
Pr-CTEN 10 pixel points	11.66	14.78	8.32	11.84
Pr-CTEN 100 pixel points	7.72	8.58	5.65	6.43
Tr-CTEN 10,000 pixel points	3.75	3.85	2.87	2.98
Meta-CTEN (proposed) 5 pixel points	5.12	4.94	3.84	4.17
Meta-CTEN (proposed) 10 pixel points	4.55	4.32	3.05	3.08

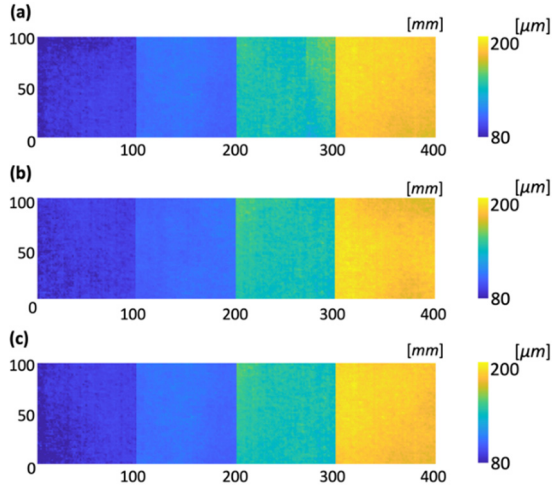

Fig. 11 Visualizing the coating thickness estimation of the white-colored acrylic type specimen: (a) Meta-CTEN, 10-pixel points; (b) Pr-CTEN, 100 pixel points; and (c)Tr-CTEN, 10,000 pixel points

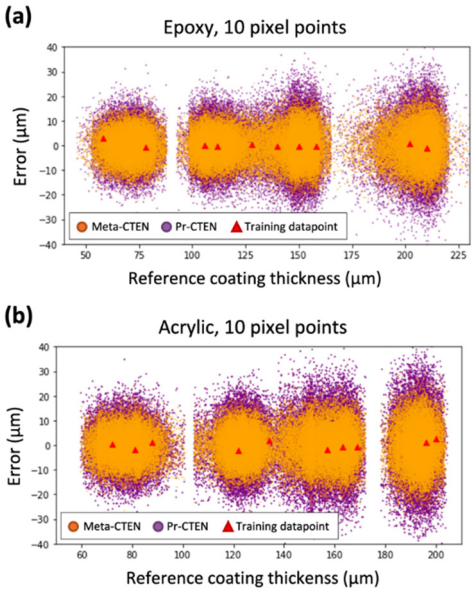

Fig. 12 Coating thickness estimation error at 10 pixel points condition: (a) Epoxy type; and (b) Acrylic type

shows a more similar pattern than that of Pr-CTEN when compared to the result of Tr-CTEN. When 10-pixel points were used for training both methods, the MAE of the Pr-CTEN model was 242% higher than that of the Meta-CTEN model, as shown in Table 1.

Fig. 12 shows the estimation error of the coating thickness after training with 10 data points. In both Meta-CTEN and Pr-CTEN, the smallest error was observed when the coating thickness was small, and it tended to increase as the coating thickness increased. In terms of coating materials, the estimation error of the pretrained CTEN model is higher than that of the Meta-CTEN model, regardless of the coating material type and color.

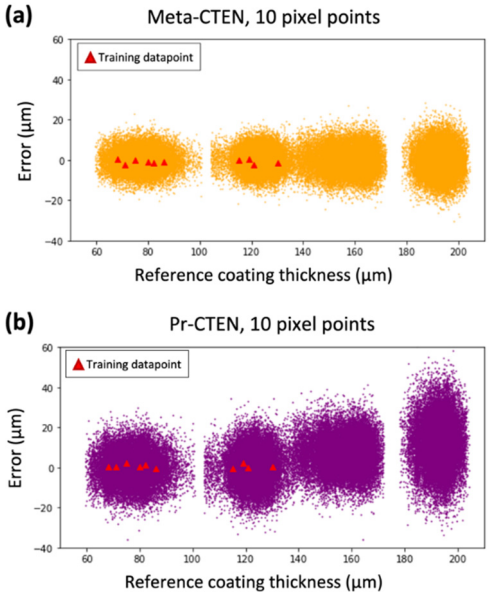

Fig. 13 Coating thickness estimation error under unbalanced pixel points condition at white-colored acrylic type: (a) Meta-CTEN with 10 pixel points; and (b) CTEN (pretrained) with 10 pixel points

The coating thickness estimation accuracy of Meta-CTEN and Pr-CTEN showed clear differences when training was performed with pixel points selected from a limited area of the specimens. Fig. 13 compares the MAE of the two methods when the pixel points are lopsided with the thin coating thickness of the specimens. Although the Meta-CTEN model was trained with only 10-pixel points selected from a thinly coated area, it correctly estimated the coating thickness of the entire structure. However, the Pr-CTEN model showed a higher estimation error despite using the same pixel points. The results indicate that the Meta-CTEN model can more reliably estimate coating thicknesses outside the input range than the Pr-CTEN model.

3.3 Field test

A field test was conducted at the Seongsan Grand Bridge, crossing the Han River in Seoul, South Korea, as shown in Fig. 14(a). The entire length of the steel truss bridge is 1,040 m and the span length is 27 m. The bridge was completed in 1980 and has been exposed to high humidity conditions for decades. Therefore, it is quite probable that not only the coating applied to the structure but also the structure itself may have been gradually damaged. Thus, a coating thickness diagnosis becomes necessary to secure the structural integrity of the bridge. The coating maintenance was partially completed; however, the coating conditions of the remaining bridge surface must be monitored closely.

The test was performed at two locations indicated in Fig. 14(a). Test location 1 was on the ground and at the intersection of the three roadways. Because the location is surrounded by layered structural members of the bridge, the influence of wind and sunlight, as well as the daily variation in temperature and humidity, are minimal. Test location 2 is

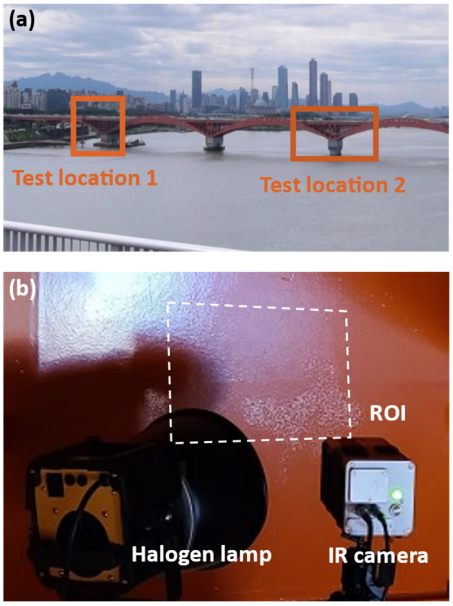

Fig. 14 Overview of the field test. (a): panoramic view of the target bridge; (b) halogen thermography system for the field test

located in the middle of the bridge, and no structural member protects the location from the external environment. Therefore, there is significant daily variation in temperature and humidity owing to the effects of wind and sunlight. Because of the environmental differences, the coating material deteriorated noticeably differently at the two test locations. At each location, three localized areas were selected for the coating thickness estimation. The three regions of interests (ROIs) at test location 1 were denoted as ROI-1, ROI-2, and ROI-3, whereas ROI-4, ROI-5, and ROI-6 represent the three ROIs at test location 2.

The halogen lamp and IR camera were positioned in front of the ROIs of the target structure, as shown in Fig. 14(b). Because of the low temperature at the test site, the distance between the halogen lamp and the surfaces of the ROIs was adjusted such that the surfaces could be heated easily. The halogen lamp was angled at 30 °from the normal line of the surface, and the IR camera was placed at the center of the specimen. All test parameters were identical to those of the lab-scale test described in Section 3.1, with the exception of a 30 s monitoring time to generate sufficient heat energy on the specimen of the target structure. This is because the test was conducted outdoors, and the temperature change owing to the halogen lamp was smaller than that in the laboratory. To fine-tune Meta-CTEN, heat responses at 10 pixel points randomly selected from ROI-1 were measured using a halogen thermography system. Validation was performed at the six ROIs after fine-tuning the proposed model. The reference coating thicknesses at the pixel points were also measured using a contact-type sensor, as in the lab-scale test. The range of the reference coating thickness for the pixel points was 180–210 μm, indicating that even in a single ROI, the coating thickness was uneven. Therefore, the average reference coating thickness at each ROI was calculated by computing the mean coating thickness of 20 randomly distributed points. In the field test, the minimum coating thickness is 146 μm and the maximum coating thickness is 512 μm.

Fig. 15 shows examples of ROI surface and the visualized images of coating thickness estimated from the proposed method. In contrast to the lab-scale test, the estimation result could be affected by wind, temperature variation, and surface deterioration of the ROIs. Nonetheless, as shown in the figure, the proposed method exhibits stable estimation performance in the presence of unfavorable external conditions. In addition, the unevenness of the coating thickness is not visible to the naked eye, but is apparent in the visualized images.

Table 2 summarizes the average and standard deviation of the coating thickness estimated using the Meta-CTEN model and the reference coating thickness measured using the contact-type sensor. The average MAE of the proposed method for the coating thickness estimation was 11 μm when compared with the average reference coating thickness on the ROI. Even though the coating material on the ROIs in the field test was degraded by wind, temperature, and sunlight for a long time, the accuracy

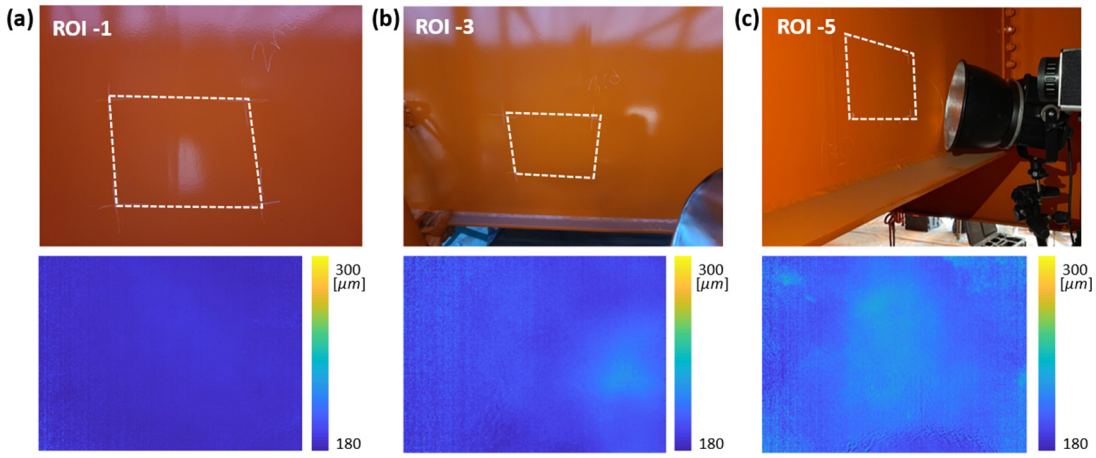

Fig. 15 Coating thickness estimation and visualization results by Meta-CTEN with 10 pixel points: (a) ROI-1; (b) ROI-3; and (c) ROI-5

Table 2 Coating thickness estimation results

Test location 1				
ROI		ROI-1	ROI-2	ROI-3
Meta-CTEN 10 pixel points	Average thickness (μm)	247.4	268.6	288.5
	Standard deviation (μm)	32.45	21.68	41.44
Reference (contact-type sensor)	Average thickness (μm)	235.3	253.5	277.6
	Standard deviation (μm)	20.30	11.14	23.85
E_{est} (%)		5.14	5.95	3.92
Test location 2				
ROI		ROI-4	ROI-5	ROI-6
Meta-CTEN 10 pixel points	Average thickness (μm)	268.3	312.5	272.3
	Standard deviation (μm)	24.52	32.58	16.48
Reference (Contact-type sensor)	Average thickness (μm)	279.3	299.0	281.7
	Standard deviation (μm)	15.34	19.52	12.11
E_{est} (%)		3.22	3.84	1.91

corresponds to E_{est} of 4.11%, which is only 1% higher than the accuracy calculated in the lab-scale test. Considering that environmental factors can cause minor variations in the physical and chemical characteristics of the coating material and structural members, and that these variations can affect the thermal response of the ROIs, it can be concluded that the proposed method estimates the coating thickness in a stable and reliable manner in the presence of surface contamination and modification of physical characteristics.

4. Conclusions

This study proposed a coating thickness estimation method for steel structures based on model-agnostic meta-learning using thermography data. Because the proposed method can estimate the coating thicknesses of various structures with only a few pixel points less than 10, the convenience and application range of the proposed method are much higher than those of the current methods. In addition, the estimation performance of the proposed method is so stable that it can be applied to thickness estimation of different coating materials. The accuracy of the proposed method was validated through lab-scale as well as field-scale tests, and the test results revealed that the proposed method can estimate the coating thickness of target structures with an accuracy of 5%, regardless of the type of coating material.

A limitation of the proposed method is that coating thickness greater than 500 μm cannot be properly estimated, since thermal energy from the halogen lamp of the proposed system is not sufficient to raise the surface temperature properly. The authors plan to expand this study to include the autonomous optimization of heating and cooling times based on external conditions. The authors' experience in the field test demonstrates that longer heating and shorter cooling times are necessary under low-temperature conditions, and that its optimization is significant for expanding the application of the proposed method.

Acknowledgments

This work was supported by a National Research Foundation of Korea (NRF) grant funded by the Korean government (MSIT) [Grant Number 2019R1A3B3067987].

References

A.A.o.S.a.H.T. Officials (Ed.) (2019), Standard Practice for Evaluation of Coating Systems for Structural Steel.

Avci, O., Abdeljaber, O. and Kiranyaz, S. (2022), "Structural damage detection in civil engineering with machine learning: Current state of the artzz", *Proceedings of the Society for Experimental Mechanics Series*, pp. 223-229. https://doi.org/10.1007/978-3-030-75988-9_17.

Beamish, D. (2004), "Using ultrasonic coating thickness gauges", *Mater. Perform.*, **43**, 30-33.

Bu, C., Tang, Q., Liu, Y., Yu, F., Mei, C. and Zhao, Y. (2016), "Quantitative detection of thermal barrier coating thickness based on simulated annealing algorithm using pulsed infrared thermography technology", *Appl. Thermal Eng.*, **99**, 751-755. https://doi.org/10.1016/J.APPLTHERMALENG.2016.01.143

Chauchard, F., Cogdill, R., Roussel, S., Roger, J.M. and Bellon-Maurel, V. (2004), "Application of LS-SVM to non-linear phenomena in NIR spectroscopy: development of a robust and portable sensor for acidity prediction in grapes", *Chemomet. Intell. Lab. Syst.*, **71**(2), 141-150. https://doi.org/10.1016/j.chemolab.2004.01.003

Cheng, W. (2017), "Thickness measurement of metal plates using swept-frequency eddy current testing and impedance normalization", *IEEE Sensors Journal*, **17**(14), 4558-4569.

Darban, S., Tehrani, H.G. and Karballaeezadeh, N. (2020), "Presentation a new method for determining of bridge condition index by using analytical hierarchy process". https://doi.org/10.20944/PREPRINTS202003.0420.V1

Farrar, C.R. and Worden, K. (2012), *Structural health monitoring: a machine learning perspective*, John Wiley & Sons.

Finn, C., Abbeel, P. and Levine, S. (2017), "Model-agnostic meta-learning for fast adaptation of deep networks", *Proceedings of the 34th International Conference on Machine Learning, ICML 2017*, **3**, 1856-1868.

Flah, M., Nunez, I., Ben Chaabene, W. and Nehdi, M.L. (2021), "Machine learning algorithms in civil structural health

monitoring: A systematic review", *Arch. Computat. Methods Eng.*, **28**(4), 2621-2643. https://doi.org/10.1007/S11831-020-09471-9

Giurlani, W., Berretti, E., Innocenti, M. and Lavacchi, A. (2019), "Coating thickness determination using X-ray fluorescence spectroscopy: Monte Carlo simulations as an alternative to the use of standards", *Coatings*, **9**(2), 79. https://doi.org/10.3390/COATINGS9020079

Goulet, J.A. (2020), *Probabilistic Machine Learning for Civil Engineers*, MIT Press.

Hahnloser, R.H., Sarpeshkar, R., Mahowald, M.A., Douglas, R.J. and Seung, H.S. (2000), "Digital selection and analogue amplification coexist in a cortex-inspired silicon circuit", Nature, **405**(6789), 947-951. https://doi.org/10.1038/35016072

Hwang, S., Kim, H., Lim, H.J., Liu, P. and Sohn, H. (2022), "Automated visualization of steel structure coating thickness using line laser scanning thermography", *Automat. Constr.*, **139**, 104267. https://doi.org/10.1016/J.AUTCON.2022.104267

I.a.T.o.S.K. Ministry of Land (Ed.) (2019), "Detailed Guidelines for Safety and Maintenance of Facilities."

Kingma, D.P. and Ba, J. (2015), "Adam: A method for stochastic optimization", *Proceedings of the 3rd International Conference on Learning Representations*, *ICLR 2015 - Conference Track Proceedings*, Vol. 1, pp. 448-456.

Standard, N.O.R.S.O.K. (2012), "Surface preparation and protective coating", NORSOK M-501, Norway.

Moskovchenko, A., Vavilov, V., Švantner, M., Muzika, L. and Houdková, Š. (2020), "Active IR thermography evaluation of coating thickness by determining apparent thermal effusivity", *Materials*, **13**(18). 10.3390/MA13184057

Muzika, L. and Švantner, M. (2020), "Flash pulse phase thermography for a paint thickness determination", *IOP Conference Series*: *Mater. Sci. Eng.*, **723**(1), 012021. https://doi.org/10.1088/1757-899X/723/1/012021

Ochiai, S., Iwamoto, S., Nakamura, T. and Okuda, H. (2007), "Crack spacing distribution in coating layer of galvannealed steel under applied tensile strain", *ISIJ Int.*, **47**(3), 458-465. https://doi.org/10.2355/isijinternational.47.458

Pan, S.J. and Yang, Q. (2010), "A survey on transfer learning", *IEEE Transact. Knowledge Data Eng.*, **22**(10), 13451359. https://doi.org/10.1109/TKDE.2009.191

Paszke, A., Gross, S., Massa, F., Lerer, A., Bradbury, J., Chanan, G., Killeen, T., Lin, Z., Gimelshein, N., Antiga, L. and Desmaison, A. (2019), "Pytorch: An imperative style, high-performance deep learning library", *Adv. Neural Inform. Processing Systems*, 32.

Reich, Y. (1997), "Machine learning techniques for civil engineering problems", *Comput.-Aided Civil Infrastr. Eng.*, **12**(4), 295-310. https://doi.org/10.1111/0885-9507.00065

Russe, I.S., Brock, D., Knop, K., Kleinebudde, P. and Zeitler, J.A. (2012), "Validation of terahertz coating thickness measurements using X-ray microtomography", *Molecul. Pharmaceut.*, **9**(12), 3551-3559. https://doi.org/10.1021/MP300383Y

Shen, H.K., Chen, P.H. and Chang, L.M. (2013), "Automated steel bridge coating rust defect recognition method based on color and texture feature", *Automat. Constr.*, **31**, 338-356. https://doi.org/10.1016/J.AUTCON.2012.11.003

Shrestha, R. and Kim, W. (2017), "Evaluation of coating thickness by thermal wave imaging: A comparative study of pulsed and lock-in infrared thermography–Part I: Simulation", *Infrared Phys. Technol.*, **83**, 124-131. https://doi.org/10.1016/J.INFRARED.2017.04.016

Wang, H., Hsieh, S.J., Peng, B. and Zhou, X. (2016), "Non-metallic coating thickness prediction using artificial neural network and support vector machine with time resolved thermography", *Infrared Phys. Technol.*, **77**, 316-324. https://doi.org/10.1016/j.infrared.2016.06.015

Zhang, J.Y., Meng, X.B. and Ma, Y.C. (2016), "A new measurement method of coatings thickness based on lock-in thermography", *Infrared Phys. Technol.*, **76**, 655-660. https://doi.org/10.1016/j.infrared.2016.04.028

Zhang, J., Cho, Y., Kim, J., Malikov, A.K.U., Kim, Y.H., Yi, J.H. and Li, W. (2021), "Non-destructive evaluation of coating thickness using water immersion ultrasonic testing", *Coatings*, **11**(11), 1421. https://doi.org/10.3390/COATINGS11111421

HJ